TEMPERATURE PROFILES FOR AN AIR TO WATER HEAT PUMP COUNTERFLOW CONDENSER

M. B. ABDUL WAHAB

SUMMARY: Experimental investigations have been made on the refrigerant-water counterflow condenser section of a small air-water heat pump. The condenser consisted of 15 meters of a thermally coupled pair of copper pipes, one containing the R_{12} working fluid and the other water flowing in the opposite direction. Thermocouples were inserted in both pipes at one meter intervals and transducers for measuring pressure and fluid flow rate were also included. Readings were taken under variety conditions; air temperature ranging from 18 to 26 degree Celsius, water inlet temperature from 13.5 to 21.7 degrees, R_{12} inlet temperature from 61 to 82 degrees and water mass flow rate from 6.7 to 32.9 grams per second. Temperature profiles and other related parameters have been predicted and compared with experimental values. The model gives a satisfactory prediction of the physical behavior.

Key Word: Heat pump condenser.

INTRODUCTION

A small laboratory air-water heat pump with heat output in the region of 1.2 kW comprises of four major components; a compressor, an evaporator, a condenser and a thermostatic expansion valve. The heat can be pumped via the evaporator coil from a lower grade energy to a higher grade energy, so that its output becomes useful for heating purposes.

The condenser comprises of a 15 meter long double-pipe, thermally coupled, in which freon and water flow in opposite directions. The physical properties of the working fluids are detected by the sensors placed at various test-points. The thermocouples for sensing temperature both the freon and water are fixed, opposite each other at one meter intervals, while four pressure transducers are placed at the inlet and at the exit of the heat pump evaporator and condenser. The water mass flow rate are measured manually.

These parameters are used to predict the thermodynamic and other physical behavior of the fluids during the process.

The heat transfer and pressure drop analysis are considered as the effect of the single-phase and two-phase flow. These effects are discussed and empirically correlated in terms of dimensionless Nusselt Number and friction factor respectively.

The research was carried out at the Heat Pump Laboratory, University of Aston in Birmingham, England. The work comprises; construction, calibration and test-sections mounting of the sensors, heat pump system, experimental measurements, computer simulation and modeling.

EXPERIMENTAL SET-UP

The air-water heat pump was modified with 180 degree-bends at every half-meter to make up the total length of 15 meter as shown in Figure 1. The experimental data obtained from the system was digitized through analog to digital converter (ADC) via an IEEE-488 interface and computer system. Thirty-two thermocouples were Positioned in the condenser, 2 were placed at the entry and exit of heat pump evaporator and one for room temperature measurements. Four pressure transducers were each placed at the entry and exit of the heat pump condenser and evaporator (Figure 1). The water mass flow rate was mechanically measured.

Figure 2 shows the cross-section of the condenser in which the thermocouples are fixed opposite to each other at the bend.

*From Department of Physics, University Pertanian Malaysia, 43400 Serdang, Selangor, Malaysia.

Figure 1: Block diagram showing the thermocouples and pressure transducers in heat pump system.

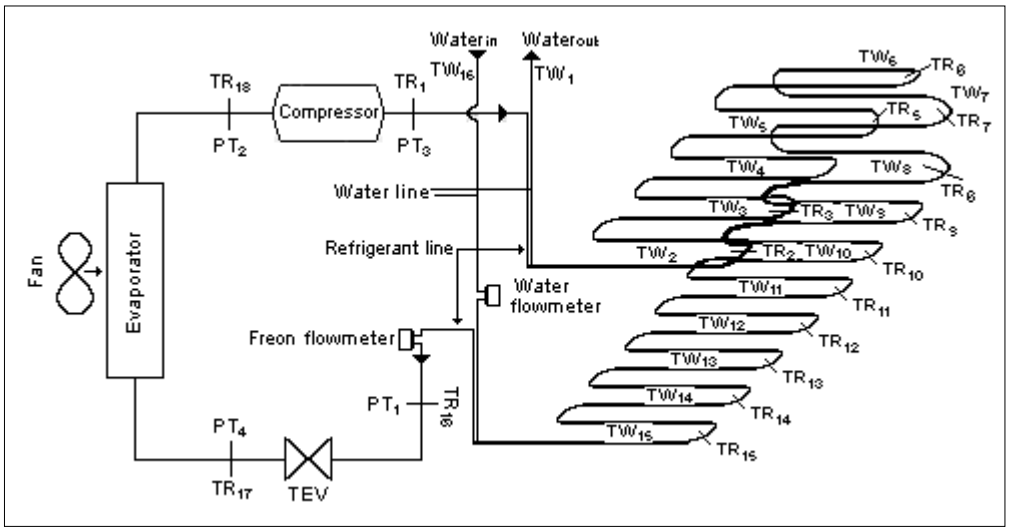

TR and TW: Freon and water thermocouple; PT: Pressure transducer; Number 1 to 18: Position at different places.

Figure 2: The partly cross-section (side view) of the DCCC condenser used in the heat pump system.

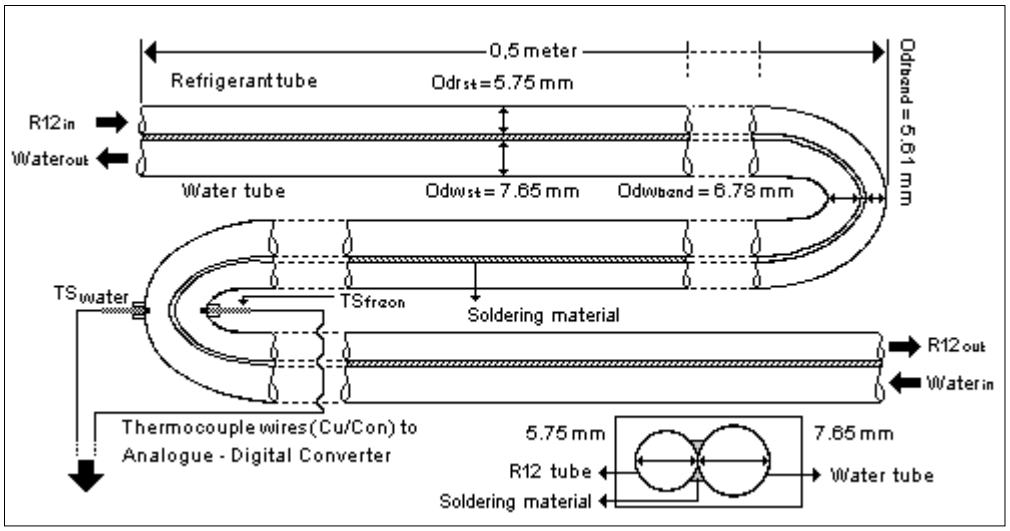

A basic program for data acquisition system was developed to store the data automatically and displayed it on the screen. A delay time between each run is set to enable the equilibrium conditions be achieved. Figure 3 shows a data acquisition system which enables the information be read and displayed automatically. Two ADC versions PCI 1001 (for channel number, CN=1 to CN=19 and CN=32 to CN=35) and PCI 1002 (for channel number CN=20 to CN=31) were used to allocate the sensors (Figure 4).

The thermocouples and pressure transducers mounting system are shown in Figures 5a and 5b.

MEASUREMENTS

Three types of calibrating-experiments had been carried out as follows,

i. Thermocouple calibration to convert ADC bits to temperature in degree Celsius.

ii. Pressure transducer calibration to convert ADC bits to absolute pressure in bar.

iii. Water flow rate measurement by conventional method to calculate mass flow rate in gram per second.

These parameters would be used to calculate the following secondary parameters,

Figure 3: A block diagram showing data acquisition for the heat pump system.

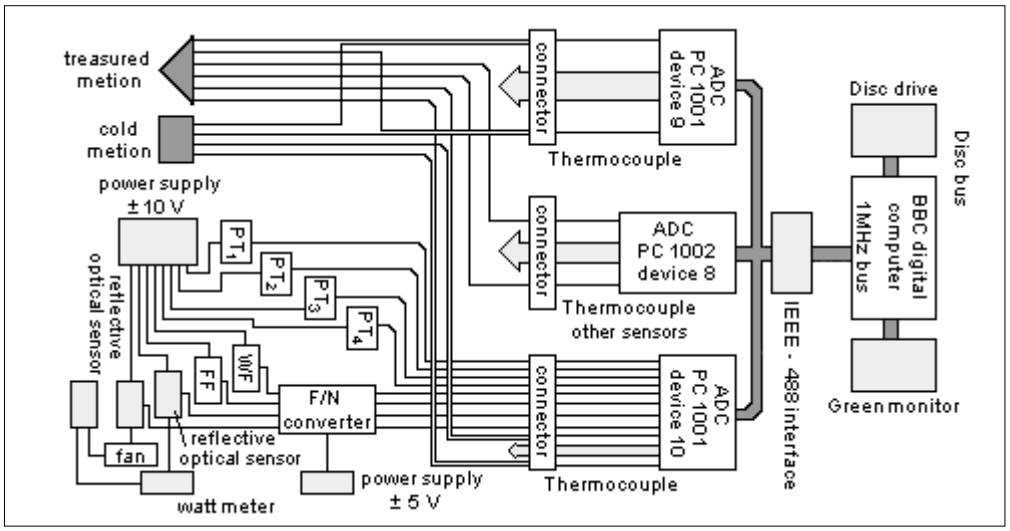

Figure 4: Sensors connecting via input ADC and an IEEE interface to digital-computer.

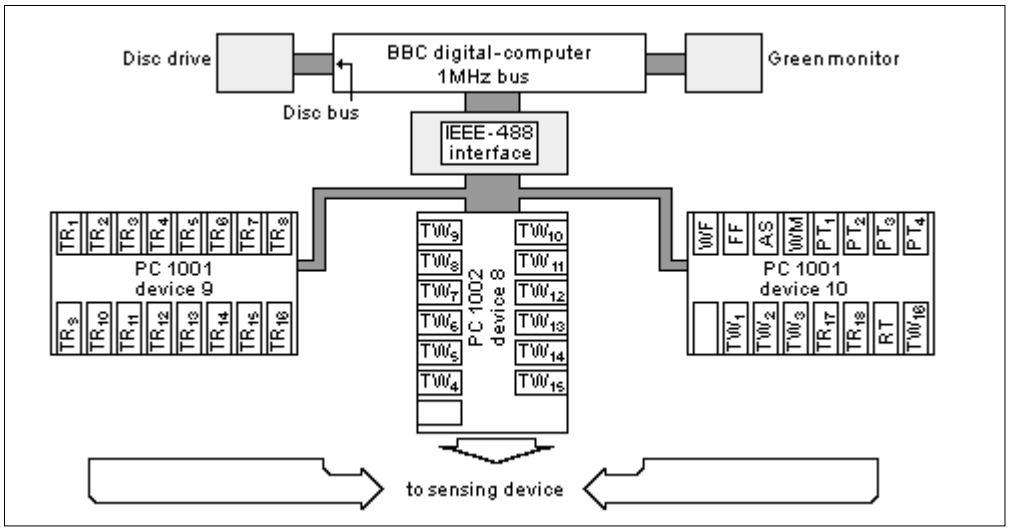

i. Freon mass flow rate, thermal power, condenser energy balance and effective inlet and outlet pressure.

ii. Thermodynamic properties of R_{12} and water at given pressure.

iii. Heat transfer coefficients for both fluids and pressures at the test-sections.

The calibration are shown in Figures 6a and 6b for temperatures using basic relationship between the bits and temperature,

$$\text{bits} = \sum_{i}^{n} a_i \ddot{A} T_i$$

where n and i are integers and ΔT = (Tmeasured-Treference); for simplicity, a second order polynomial was considered. A least square curve fitting program was used to calculate the calibration coefficients.

The comparison between the measured and the calculated temperatures is shown in Tables 1a and 1b. For the pressure, a linear relationship between the bits and pressures was considered. The measured and the calculated pressure was compared and shown in Figures 7a and 7b.

Figure 5a: Thermocouples mounting system in water and refrigerant line.

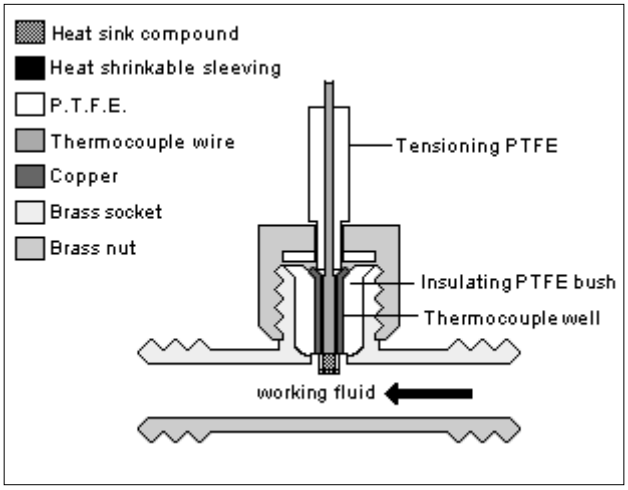

Figure 5b: Static pressure transducer in live with the thermocouple mounting system in R_{12} line.

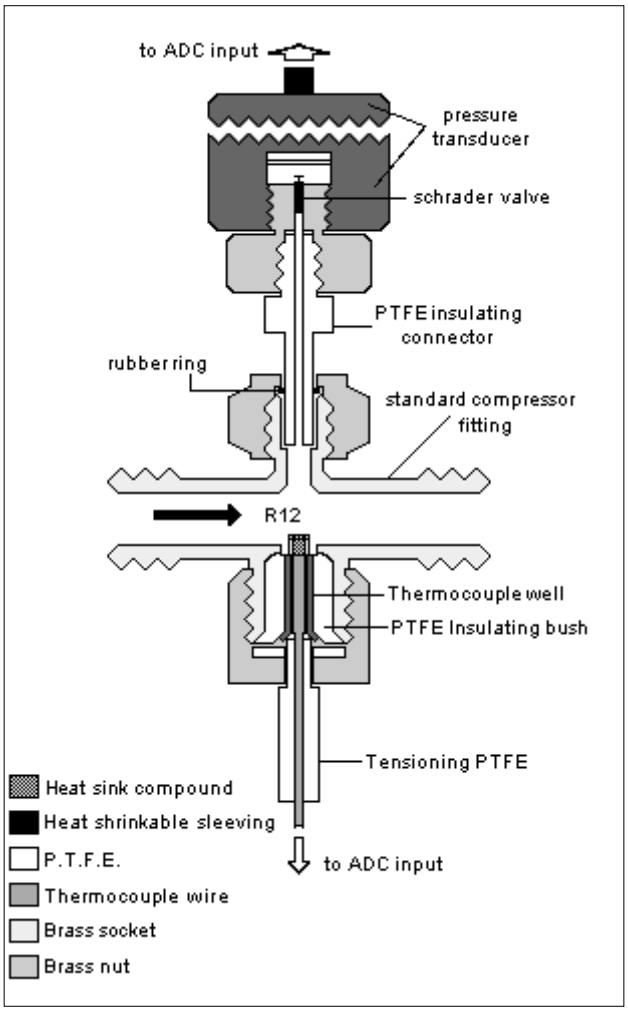

ERROR ANALYSIS IN CALIBRATION

There are two main sources of error encountered in the measurement. Firstly, due to human factor in reading from the conventional device or in the device itself when registering the measured parameters. Secondly, the digitizing error that may occur during the analog digital conversion.

Figure 6a: Measured temperature versus bits for CN=1 to CN=19 and CN=32 to CN=35 (PCI 1001).

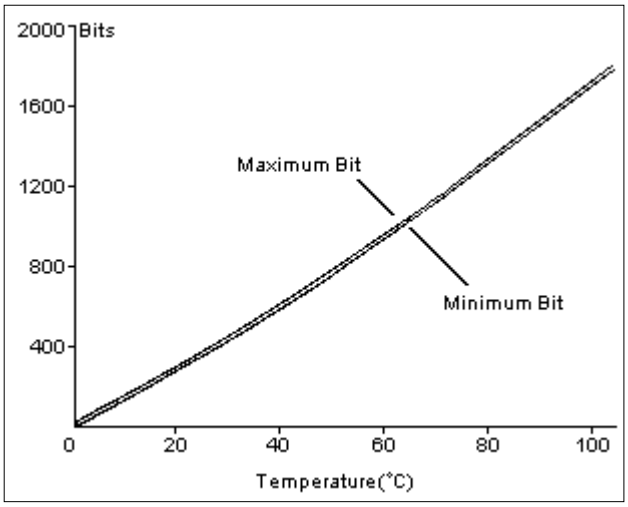

Figure 6b: Measured temperature versus bits for CN=20 to CN=31 (PCI 1002).

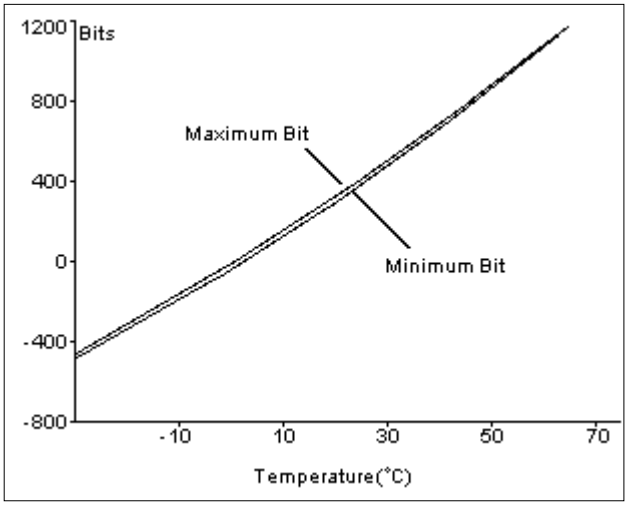

Thermocouples

The conventional thermometer for temperature calibration was capable of measuring to an accuracy of 0.1°C. Due to difficulty in visualizing exactly between step marked on the thermometer glass, that would bring to a

Table 1a: Comparison between the measured and the calculated temperatures for CN=1 to CN=19 and CN=32 to CN=35.

CN	Measured temperature (°C)										
	0.00	9.00	20.70	31.40	39.50	44.80	52.30	62.10	69.50	76.40	90.70
	Calculated temperatures for CN=1 to CN=19 and CN=32 to CN=35 in (°C)										
1	0.06	8.97	20.53	31.39	39.66	44.85	52.42	61.98	69.54	76.21	90.80
2	0.07	8.98	20.49	31.38	39.67	44.85	52.43	61.97	69.57	76.19	90.79
3	0.10	8.96	20.45	31.35	39.70	44.90	52.43	61.98	69.58	76.14	90.81
4	0.09	8.99	20.43	31.35	39.71	44.89	52.45	61.97	69.59	76.11	90.82
5	0.08	9.00	20.44	31.36	39.71	44.88	52.42	61.96	69.58	76.17	90.80
6	0.06	9.02	20.44	31.38	39.70	44.87	52.40	61.98	69.56	76.18	90.80
7	0.04	9.02	20.49	31.39	39.68	44.86	52.39	62.00	69.52	76.21	90.80
8	0.07	8.98	20.48	31.39	39.70	44.86	52.41	61.99	69.53	76.19	90.80
9	0.07	8.98	20.48	31.40	39.68	44.87	52.40	61.99	69.54	76.20	90.80
10	0.07	8.99	20.45	31.39	39.69	44.87	52.40	61.99	69.56	76.26	90.77
11	0.08	8.97	20.49	31.39	39.67	44.86	52.38	61.97	69.55	76.26	90.77
12	0.04	9.00	20.53	31.38	39.66	44.86	52.38	61.96	69.54	76.26	90.78
13	0.04	8.99	20.55	31.40	39.63	44.87	52.35	61.99	69.51	76.32	90.75
14	0.03	8.99	20.54	31.44	39.63	44.87	52.37	61.98	69.47	76.31	90.78
15	0.05	8.98	20.53	31.42	39.65	44.87	52.36	61.99	69.50	76.28	90.78
16	0.03	9.01	20.51	31.43	39.64	44.86	52.36	62.00	69.50	76.29	90.77
17	0.00	9.02	20.60	31.38	39.65	44.84	52.31	62.01	69.53	76.31	90.76
18	0.02	9.02	20.54	31.38	39.66	44.85	52.36	62.01	69.56	76.22	90.79
19	0.04	9.01	20.54	31.37	39.66	44.84	52.36	62.01	69.56	76.23	90.78
32	0.02	9.03	20.51	31.43	39.64	44.84	52.35	62.00	69.51	76.30	90.76
33	0.03	8.99	20.56	31.44	39.62	44.84	52.33	62.00	69.49	76.35	90.75
34	0.02	8.97	20.67	31.42	39.57	44.82	52.30	62.02	69.47	76.43	90.72
35	0.01	8.98	20.65	31.41	39.60	44.84	52.31	61.99	69.46	76.44	90.72

Table 1b: Comparison between the measured and the calculated temperatures for CN=20 to CN=31.

CN	Measured temperature (°C)										
	0.00	9.00	20.70	31.40	39.50	44.80	52.30	62.10	69.50	76.40	90.70
	Calculated temperatures for CN=20 to CN=31 in °C										
20	0.06	9.07	20.63	31.37	39.63	44.86	52.35	61.89	69.54	76.22	90.76
21	0.04	9.07	20.67	31.38	39.62	44.85	52.31	61.89	69.50	76.33	90.73
22	0.08	9.06	20.63	31.35	39.63	44.87	52.35	61.89	68.54	76.27	90.73
23	0.09	9.06	20.57	31.33	39.67	44.88	52.38	61.90	69.58	76.13	90.78
24	0.09	9.05	20.58	31.35	39.66	44.89	52.36	61.89	69.59	76.13	90.78
25	0.09	9.05	20.58	31.36	39.65	44.89	52.36	61.90	69.58	76.14	90.78
26	0.05	9.07	20.61	31.39	39.65	44.84	52.34	61.92	69.55	76.16	90.79
27	0.07	9.09	20.57	31.35	39.67	44.84	52.37	61.94	69.54	76.17	90.79
28	0.10	9.05	20.55	31.35	39.67	44.89	52.38	61.91	62.56	76.12	90.79
29	0.10	9.06	20.54	31.36	39.68	44.89	52.36	61.90	69.56	76.15	90.79
30	0.10	9.06	20.54	31.34	39.67	44.90	52.39	61.88	69.57	76.15	90.78
31	0.09	9.06	20.59	31.34	39.64	44.87	52.38	61.91	69.56	76.21	90.77

Figure 7a: Calibration curve; bits versus pressure.

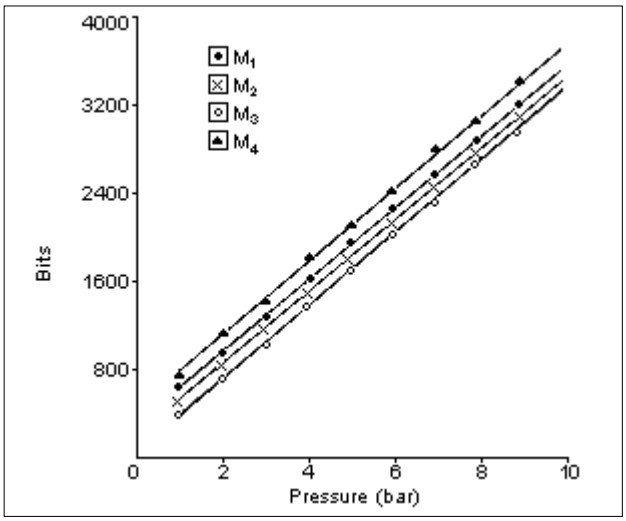

Figure 7b: Calibration curve for pressure.

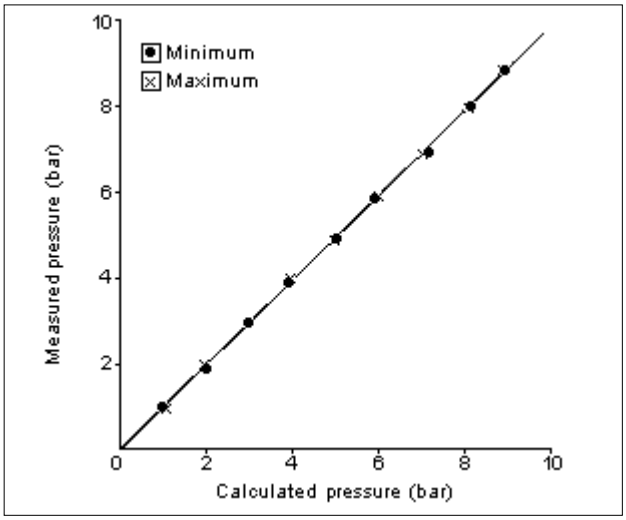

maximum of ±0.2°C error in measurement both at the measured point and reference point. Other errors that may appear could be from the thermocouples themselves. Some of them are listed below,

i. The presence of the sensor may alter the temperature field (installation error).

ii. Heat transfer would cause the temperature at the sensing element to be slightly different from the temperature of the body or temperature of the fluids at particular location-small temperature drop.

iii. The depth of immersion of the sensing element into the stream of the fluid for each thermocouple may not be the same.

iv. The temperature distribution in the sensing element may not be the same with the temperature of the fluid at that region.

v. Physical and chemical properties of the insulation used in the system must also be considered.

Pressure transducer: The pressure calibration device has claimed an accuracy of ±0.05% of the pressure being measured. At higher pressure range encountered (≥16 bar), would correspond to an uncertainty error of ±0.008 bar and at lower pressure range (≤3 bar) to an accuracy error of ±0.0015 bar.

Digitizing error: The ADC employed in the system is a 12-bit device with the full scale input voltage from -1V to +1V, represented digit by bits from -4096 bits to +4096 bits. At 0°C (cold junction), the thermocouple generates 46 μV/°C at 100°C. The digitizing errors occurring in the temperature measurement is given in Table 2. The errors may regarded as small compared to the reading from the thermometer (±0.2°C).

Table 2: Thermocouple and pressure transducer digitizing error.

ADC	Sensor	Sensitivity	Digitizing error
Differential-input	Thermocouple	19.0 bits/°C	±0.05°C/bits
Channel 3 of PCI 1002 (Differential-input)	Internal cold junction	40.0 bits/°C	±0.025°C/bits
Differential-input	Pressure	290 bits/bar	±0.0034bar/bit

Based on these results, the maximum errors occur in the temperature and pressure measurement are ±0.2°C and ±0.0082 bar respectively.

Mass flow rate measurement: The chief source of error encountered in the water mass flow rate measurement was the uncertainty due to human error in reading technical error which is difficult to quantify numerically. The possible maximum fractional error of water mass flow rate was ±0.10824 gram per second.

The freon mass flow rate calculation was determined from the considerations of the condenser energy balance equation,

$Q_{freon} = Q_{water} + Q_{loss}$

where Q_{freon} is the total thermal energy released from

the freon side which is the sum of the thermal energy picked up by the water side, Q_{water} and heat lost from the condenser, Q_{loss}.

On simplification, the freon mass flow rate can be written as,

$$m_r = \left(\frac{m_w c_{pw} \Delta TW + Q_{loss}}{\Delta h_r} \right)$$

where mw = Total water mass flow rate in Kgs^{-1}
cpw= Specific heat capacity of water (=4.1833 $Jg^{-1}°C$)
DTW = (TW_1 - TW_{16}) in °C
Dhr = ($h_{g,1}$ - $h_{f,16}$) in Jkg^{-1}
TW_1 = Condenser outlet water temperature in °C
TW_{16} = Condenser inlet water temperature in °C
$h_{g,1}$ = Specific enthalpy of vapor component at point 1
$h_{f,16}$ = Specific enthalpy of liquid component at point 16

$E_{in} = Q_{freon} - (Q_{water} + Q_{loss}) = 0$

In this case, the energy in balance could be written as,

SOFTWARE FOR DATA ACQUISITION PROGRAM

A Flowchart listed in Figure 8 was used for all Runs. The data for each Run was time averaged because of the quasi-static nature of the experimental run.

An average of ten sets of readings were taken from the thermocouples and pressure transducers sequentially. The time for acquiring data and the quantity of water being collected during this period was recorded for flow rate calculation.

RESULTS

The results within the operating conditions (as mentioned earlier) are presented. The results will be summarized from experimental analysis and predicted data.

Experiment

The experimental results cover the following operating conditions; 7.6-12.3 bar for the inlet pressure, 61.2-81.7°C for the inlet freon temperature, 13.5-21.7°C for the water inlet temperature, and 6.72-12.49 gram per second for water mass flow rate.

In general, the temperature of freon decreases over the length of heat exchanger (direction of freon's flow) and at the same time water temperature increases in the opposite direction (picked up some heat from the freon

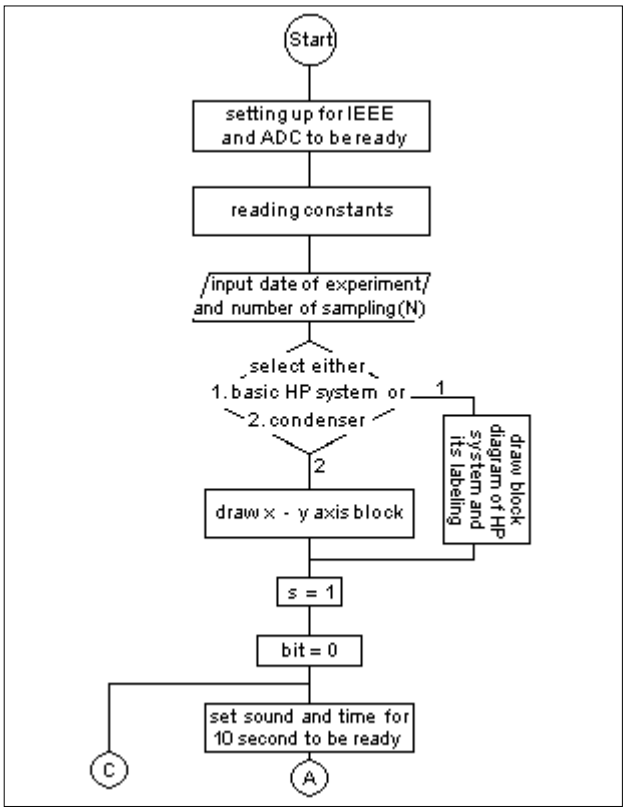

Figure 8: Flowchart description for sampling data.

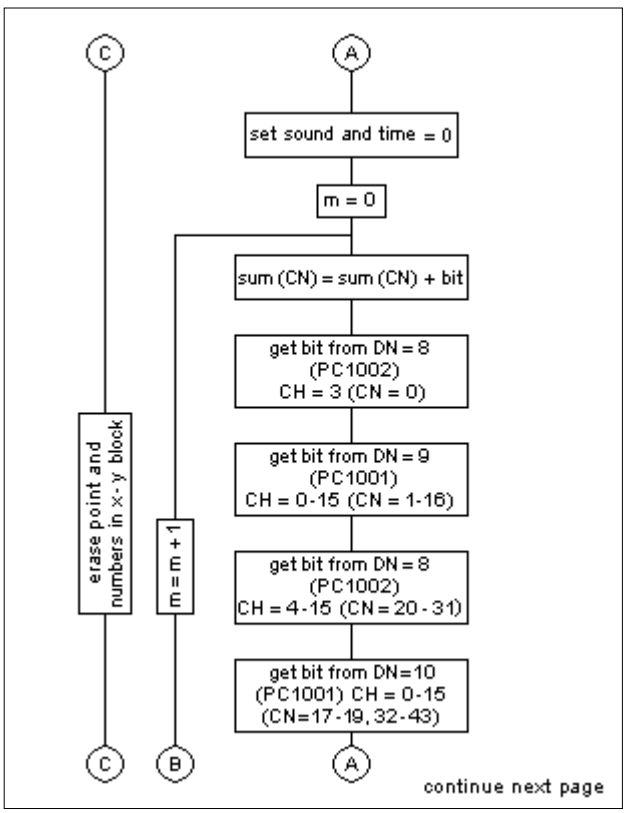

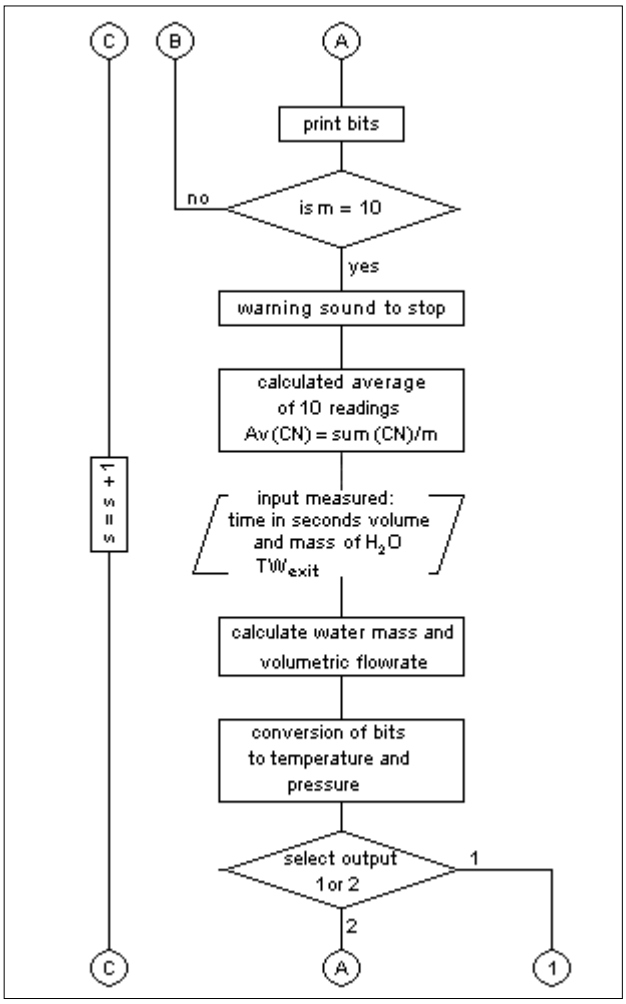

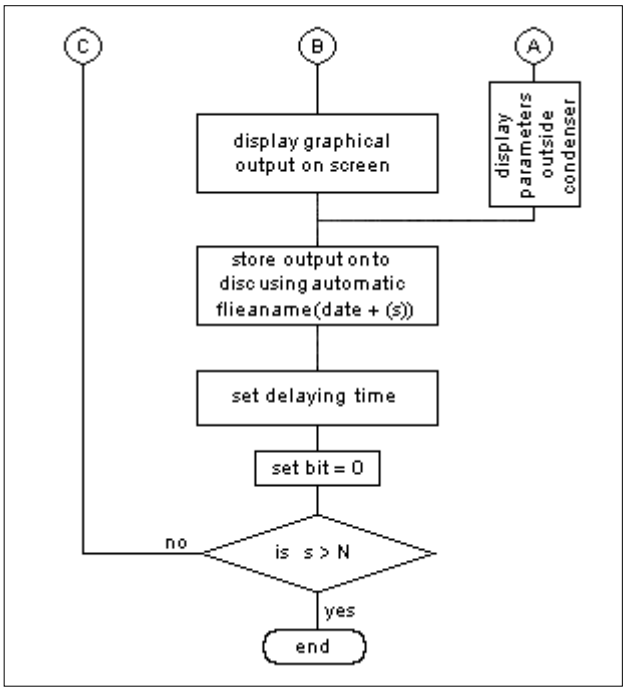

side). For higher freon inlet temperature, the inlet pressure becomes higher, and the water mass flow rate decreases. Room temperature ranged from 18°C to 26°C.

There is a sharp drop in the freon temperature in the first few meters of the condenser entry due to the pressure drop in the tube, and after that, the drop is moderate before continuing to drop as the freon flows towards the condenser exit.

The desuperheating region can be represented by the tremendous drop just after the freon flow in the condenser. The two-phase region can be represented by the small temperature drop which covers most of the condenser length. Finally, the moderate drop indicated by the few points towards the condenser exit can be regarded as the sub cooling region. At the same time, heat lost from the freon side picked-up by the water causing the water temperature to increase in the opposite direction. As the freon inlet pressure increases, the freon and water mass flow rate in decreased. The pressure drop across the condenser is between 10 bar to 15 bar.

Prediction

Some of the experimental results obtained were used as input data; total thermal power, water inlet temperature, freon inlet temperature, freon inlet pressure, and overall percentage of thermal energy lost to surroundings. Other input data assumed to have a fixed value; wall thickness of the tube, freon and water outside diameter, total length of condenser and conductivity of thermal bond between the tubes.

Temperature distribution at one meter intervals along the fifteen meter condenser were predicted by the proposed model. The temperature profiles for every 0.2 meter are shown.

Comparison between experiment and model: The temperature profiles for the freon and water along the heat pump condenser are compared with the predicted results. The results are for the freon inlet pressure and temperature from 7.65 bar to 10.89 bar and 55.4°C to 68.6°C respectively and room temperature ranged from 18.5°C to 19.5°C.

For run 5, 9, 10, 11 and 12, the temperature distribution for the freon side deviates from -1.7°C to 6.5°C, while for the water side, it deviates from -1.6°C to 0.9°C (Figures 9a and 9b). These results are graphically shown in Figure 10.

There is a sharp drop in the freon temperature

Figure 9a: Experimental and predicted temperature profile for the freon side compared (Section A of Table 6.2).

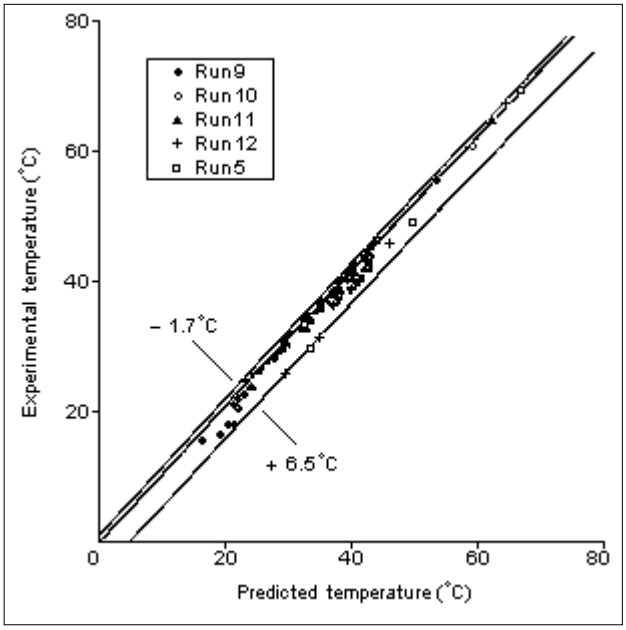

Figure 9b: Experimental and predicted temperature profile for the water side compared (Section A of Table 6.2).

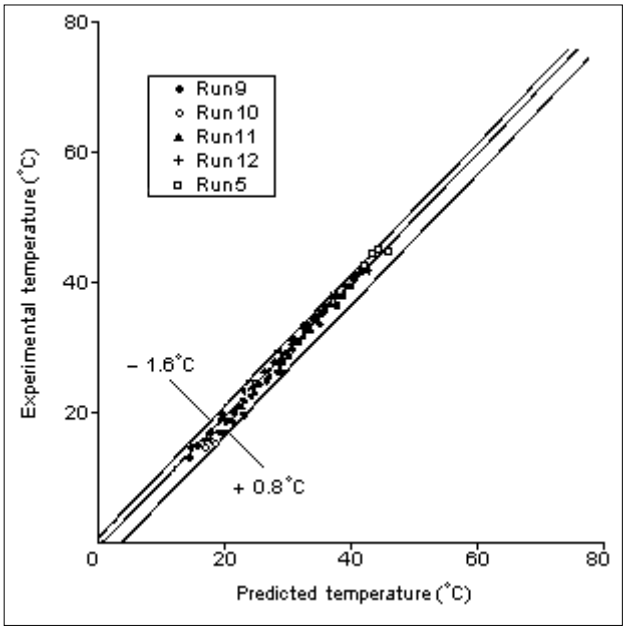

between the last point in the mixed-region and the last point in the condenser exit (subcooling region), but the drop predicted in the two-phase region is quite moderate. As the freon inlet pressure increases, the drop is moderately decreased.

Figure 10: Experimental and predicted temperature profile of section A for freon Inlet pressure 7.65-10.63 bar.

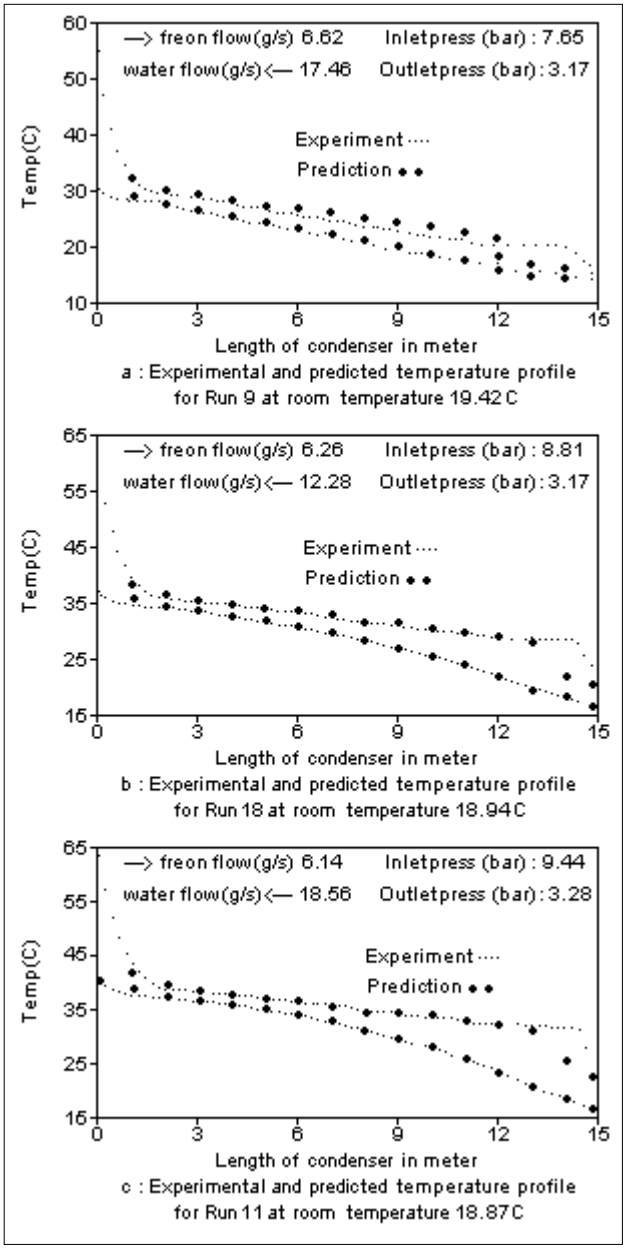

For the water side, the temperature rise can be clearly seen after the waters enters the condenser exit and flows a few meter along the condenser, and after that, the slope is gradually decreased until the water leaves the condenser entry.

CONCLUSIONS

For normal operating conditions, the model is in fairly good agreement with the experimental results. The pre-

Figure 10: Continue.

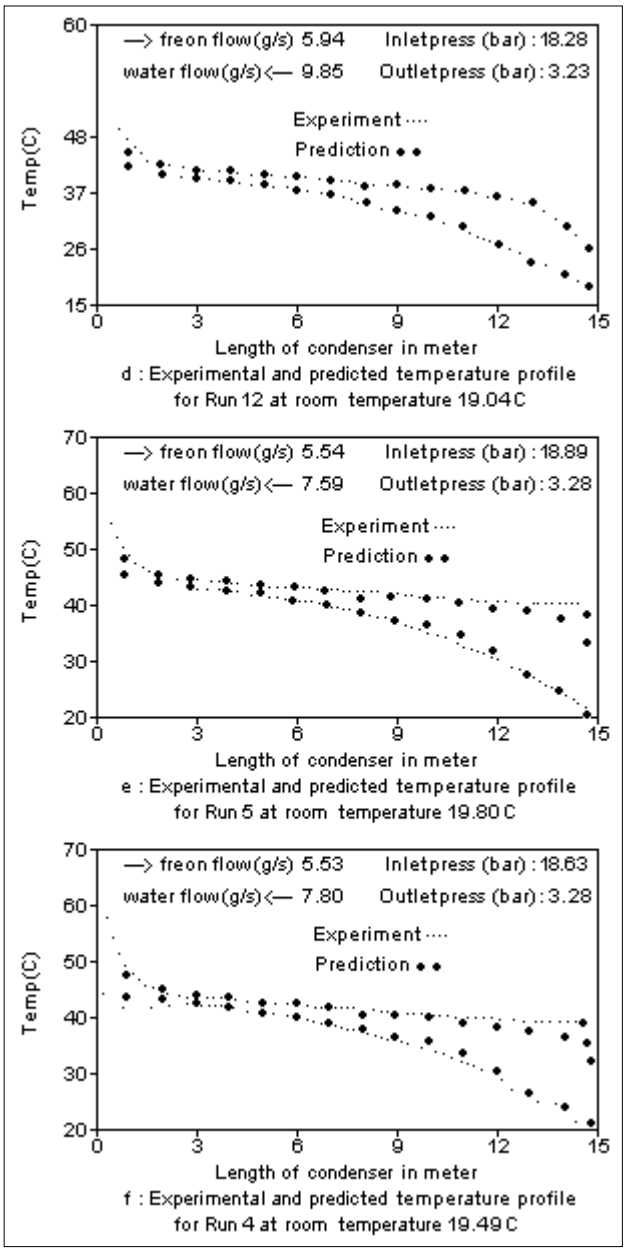

dictions for the freon side are slightly higher at the few points just before the mixture of liquid-vapor is completely condensed. For the water side, the predicted temperature profiles are almost on par with the experiment.

ACKNOWLEDGMENT

I would like to express my heart felt gratitude to Mr. C G Pearce, Dr . P N Cooper, Mr. M S Wrenn, Dr. R A Summers, and Dr D Hetherington of Department of Electrical, Electronic Engineering and Applied Physics, Aston University, Birmingham, England for encouragement, guidance, useful criticism, suggestions, and much advice throughout the course of this project.

I would also like to thank the technicians and colleagues of the Heat Pump Laboratory of Aston University, Birmingham.

REFERENCES

1. Carrington CG : Computer program of a counterflow R12 condenser comprised of two tubes thermally coupled. Unpublished, Aston Univ, Birmingham, 1982.

2. Crew M : Showing how a heat pump works. The heating of ventilating engineers, April/May, pp 22-26, 1984.

3. Lockhart RW, Martinelli RC : Proposed correlation of data for isothermal two-phase, Two-component flows in pipes. Chem Engng Progress, 45:39-45, 1949.

4. Gowen RA, Smith JW : Turbulent heat Transfer for smooth and rough surfaces. Int J Heat Transfer, 11:1657-1673, 1968.

5. Wassel AT, Mills AF : Calculation of variable property turbulent friction and heat transfer in rough pipes. Trans ASME J Heat Transfer, 101:449-474, 1979.

6. Zivi SM : Estimation of stedy-state steam void-fraction by means of the principle of minimum entropy productions. Trans ASME J Heat Tranfer, 86:27-252, 1964.

7. Martinelli RC, Boetler LM, Taylor THM, Thomson EG, Morrin EH : Pressure drop for two-component flow in a horizontal pipe. Trans ASME, pp 139-151, 1944.

8. Hickson DC : R12 thermodynamic property-computer program. Aston Univ, Birmingham, England.

9. Kay JM, Nedderman RM : Fluid mechanis and transfer processes. Cambridge Univ Press, pp 217-238, 1985.

10. Kakac S : The effect of temperature-dependent fluid properties on convective heat transfer, handbook of single-phase convective heat transfer. Ed by S Kakac, et al., Willes-Int Pub, John Wiley and Sons, Chap 18, pp 18.1-18.56, 1987.

Correspondence:
M. B. Abdul Wahab
Department of Physics,
University Pertanian Malaysia,
43400 Serdang, Selangor,
MALAYSIA.